
Wavelet GPT - Wavelet Inspired Large Language Models

Prateek Verma¹

Abstract

Large Language Models (LLMs) have ushered in a new wave of artificial intelligence advancements impacting every scientific field and discipline. We live in a world where most of the data around us, e.g., text, audio, and music, has a multi-scale structure. This paper infuses LLMs with a traditional signal processing idea, namely wavelets, during pre-training to take advantage of the structure. Without adding **any extra parameters** to a GPT-style LLM architecture in an academic setup, we achieve the same pre-training performance almost twice as fast in text, audio, and images. This is done by imposing a structure on intermediate embeddings. When trained for the same number of training steps, we achieve significant gains in performance, which is comparable to pre-training a larger neural architecture. Further, we show this extends to the Long Range Arena benchmark and several input representations such as characters, BPE tokens, bytes, waveform, math expression, and image pixels. Our architecture allows every next token prediction access to intermediate embeddings at different temporal resolutions in every decoder block. We hope this will pave the way for incorporating multi-rate signal processing into pre-training instead of going after scale.

1. Introduction and Related Work

LLMs have ushered in a super-renaissance of AI advancements and are touching every scientific and engineering discipline. At the heart of this is the Transformer architecture (Vaswani et al., 2017), initially proposed for machine translation. Transformer architecture became the backbone of GPT (Generative Pretrained Transformer) language models (Brown et al., 2020) first proposed by Open-AI. Modern LLMs are trained on a straightforward objective: To pre-

dict the next token given the previous context, preserving the causality. This not only works for language but also for robotics (Brohan et al., 2023b;a), protein sequences (Madani et al., 2020), raw audio waveforms (Verma & Chafe, 2021), acoustic/music tokens (Huang et al., 2019; Verma & Smith, 2020; Borsos et al., 2023), videos (Yan et al., 2021) etc. This simple recipe of tokenization/creating an embedding and feeding it to transformers also has given rise to non-causal architectures such as BERT (Devlin et al., 2019), Vision Transformers (Dosovitskiy et al., 2021), Audio Transformers (Verma & Berger, 2021) and Video Transformers (Selva et al., 2023). With increased performance by scale, LLMs are reaching hundreds of billions to trillions of parameters (Brown et al., 2020; Fedus et al., 2022).

Recent concerns suggest AI research is shifting from academia to industry, according to a Washington Post article by (Nix, 2024). This work aims to enhance LLM capabilities to match those of larger architectures or achieve equivalent performance in fewer training steps. Knowledge distillation (Hinton et al., 2015), uses a larger model to guide a smaller one. (Gu et al., 2024) used KL divergence to enhance next-token prediction from teacher model feedback model rather than training the smaller one from scratch. Model pruning (Sun et al., 2024) removes weights to match the same performance as a large model like LLAMA (Touvron et al., 2023), with fewer compute flops during inference, still relying on a larger model. (Dettmers et al., 2024) focus on improving inference or fine-tuning existing models. Unlike distillation and pruning our approach focuses on improving performance during pre-training from scratch. (Nawrot et al., 2022), proposed hierarchical transformers using upsampling-downsampling operations achieve results comparable to those of Transformers but with more efficient computation. Clockwork RNN (Koutnik et al., 2014) improves long-context modelling by splitting RNN neurons into modules that update at different clock rates. Only a few modules activate at each time step. Our approach modifies intermediate embeddings with simple tweaks without using separate learning modules or varying update rates.

Tinkering with the intermediate embeddings: (Tamkin et al., 2020) proposed hand-tuned filters on the Discrete Cosine Transform- DCT (Ahmed et al., 1974) of the latent space for different NLP tasks for non-causal BERT (Devlin et al., 2019). Computing DCT over context length makes

¹Department of Computer Science, Stanford Natural Language Processing Group, Stanford University, Stanford, CA 94305. This work was done while Prateek Verma was with the Stanford Natural Language Processing Group in 2023. Correspondence to: Prateek Verma <prateekv@stanford.edu>.

it not applicable for causal applications such as language modelling. There has been work on applying ideas from signal processing-like methods to BERT-like non-causal architectures. We discuss two here, FNet and WavSPA. They focus on improving attention block, which differs from our work on GPT, which retains a vanilla attention layer. FNet proposed by (Lee-Thorp et al., 2022) removes the costly attention mechanism, replacing it with a 2-D FFT block. This operation is non-causal as it looks into future tokens for computing 2-D FFT. WavSpA (Zhuang et al., 2024) carries attention mechanism in the wavelet space. The input sequences are transformed into wavelet space, and the attention mechanism is carried out and then reconstructed. However, computing wavelet transform is non-causal, making them non-applicable for GPT-based LLMs as they look at the entire sequence length (Fig 1 (Zhuang et al., 2024)).

Our work is inspired by neuroscience, which provides evidence that human brain learns multi-scale representations for language at multiple time scales (Caucheteux et al., 2023) instead of fixed-resolution representations. We impose multi-scale representation onto every intermediate decoder embedding at different dimensions. To the best of our knowledge, the paper’s contributions are: 1) We propose the first instance of incorporating wavelets into LLM pre-training. We add multi-scale filters onto each of the intermediate embeddings of decoder layers using the Haar/learnable wavelet pipeline. This allows every next token prediction access to multi-scale intermediate embeddings instead of being fixed-resolution in every decoder layer representation. 2) We show speedups in pre-training of GPT, like transformer-based LLM in the range of 40-60%, with adding a multi-scale structure. With same training steps, the model gives a performance boost akin to adding several layers.

2. Dataset

We use four open-source datasets from four domains for next token prediction: natural language, symbolic music, speech tokens, and raw audio waveform. For text, we choose text-8 (Mikolov et al., 2012). We choose this over other datasets as i)it is a famous and widely cited character-level language modelling dataset, and ii) it uses a simple vocabulary (space + 26 lowercase characters) to detach the effects of various tokenizers. It has 100M characters with split training split as given by (Al-Rfou et al., 2019). For raw audio, the goal is to predict the next sample given the context. We use the YouTube-Mix-8 dataset for long-context modeling (Goel et al., 2022; Verma, 2022). Our vocabulary size is 256, with a sampling rate 16KHz as input is 8-bit. We use a third dataset, MAESTRO (Hawthorne et al., 2019), containing over 1000 MIDI files of classical music pieces with a tokenizer proposed by (Huang et al., 2019), which converts MIDI tracks into discrete tokens with a vocabulary

size of 388. Finally, we use 1000 hours of LibriSpeech dataset and a widely used ENCODEC (Défossez et al., 2022) tokenizer in a setup similar to VALL-E (Wang et al., 2023) to model acoustic tokens¹. The goal in all four modalities is not to chase state-of-the-art pre-training performance, as *this paper was written in an academic setting with very few computational resources*. We show how the model performs in pre-training instead of post-training, as the goal is to build better foundational architectures with the same parameters, pushing the capabilities of smaller decoder architectures.

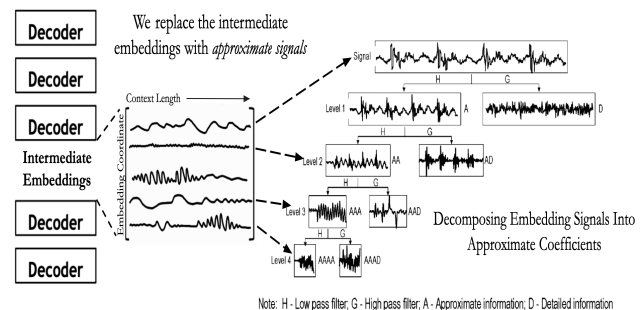


Figure 1. Manipulating signals between GPT decoder blocks by computing 1-D causal discrete haar wavelet transform/learnable approximation at different levels capturing multi-scale structure for each signal. (Right) From (Gao & Yan, 2006) explaining non-stationary signal processing for signals. Leftmost route of approximate coefficients to model coarsest to finest scales.

3. Methodology

This section will describe the approach to incorporating wavelet inspired computation into transformer-based Large Language Models while retaining causality. The ideas described here are generic as we tinker intermediate embeddings. Thus they can be easily extrapolated to non-Transformer architectures, e.g. state space model. For any GPT signal, we compute a version of the discrete wavelet transform and incorporate it back into the signal. Let $x_{(i)}^l$ be the output of the l^{th} decoder layer, representing the activation along the i^{th} coordinate, with a dimension equal to the context length L of the transformer-based GPT model. In the original GPT architecture with $N + 1$ layers and embedding dimension E , we obtain $N \cdot E$ signals of length L from intermediate embeddings between decoder blocks, where E ranges from $[0 - 128)$ dimensions. For any signal $x[n]$, the discrete wavelet transform resembles passing the signal through filters of varying resolutions, as illustrated in Figure 2. We will use the Haar wavelet, a family of square-shaped functions this paper obtained from a mother wavelet via

¹The goal in this work, is how well we can model the coarsest tokens, as errors in modelling the coarser tokens will lead to the finer tokens being modelled incorrectly as they are conditioned on the coarsest token, thus affecting model performance

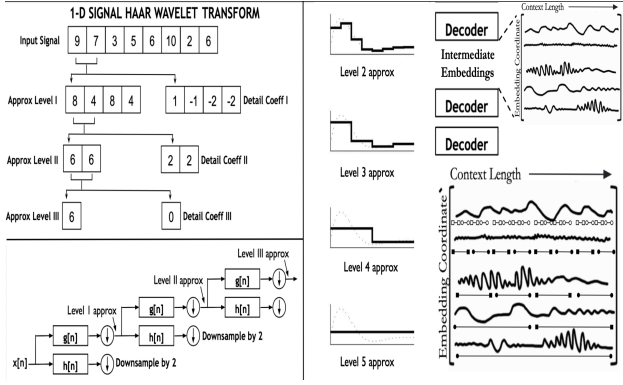


Figure 2. (Bottom L): A 3-level filter bank tree generates signals at different resolutions. Approximate coefficients are computed by applying a wavelet’s impulse response & recursively downsampling. (Top L): Approximate and detailed coefficients are iteratively calculated via first-order averages/differences and downsampling until a single scalar represents the signal. (R): For a 32-length signal, Haar wavelet captures coarsest to finest approximations and is redrawn from (Flores-Mangas, 2014). Embeddings evolve at different rates via causal wavelet approximation, with coarse (level 5) and fine (level 2) resolutions, embedding multi-scale information into decoder layers for every token.

scaling and shifting operations. Given a mother wavelet function ψ , the child wavelets as $\psi_{j,k}[n]$, where j is the scaling factor and k is the shift factor.

$$\psi_{j,k}[n] = \frac{1}{\sqrt{2^j}} \psi \left(\frac{n - k2^j}{2^j} \right) \quad (1)$$

These signals are shifted and scaled to capture information at various time scales, with n representing time or the context length. This concept resembles the diagram in Figure 1, which illustrates capturing different signals in the intermediate layers of Transformer decoders at various resolutions. Discrete wavelet transform, which passes any signal through filters and downsampling operations. This process, shown in Figure 2, is similar to a convolutional neural network (CNN) like ResNet (He et. al, 2016), featuring learned convolutional filters analogous to $h[n]$ and $g[n]$, along with downsampling, such as max pooling. In convolutional architectures, we follow one branch of Figure 2, recursively taking the output of filters and downsampling. This similarity contributed to popularity of wavelets in the 1990/2000s for image understanding, reflecting parallels with convolutional architectures (Huang & Aviyente, 2008; Kingsbury & Magarey, 1998). For Haar wavelets, this is passing the signal through low-pass and high-pass filters corresponding to the kernels $g[n]$ and $h[n]$. The Haar wavelet transform averages and computes differences, with impulse responses $g[n] = [\frac{1}{2}, \frac{1}{2}]$ and $h[n] = [\frac{1}{2}, -\frac{1}{2}]$. Figure 2 provides a detailed explanation of the discrete wavelet transform. For a 1-D signal $x[n]$ of length L , we get level 1 coefficients by filters $g[n]$ and $h[n]$, followed by downsampling. Thus, the

approximation coefficients y_{approx} and y_{detail} result from a LTI system defined by convolution followed by downsampling by two (Equation 2). This is seen in Algorithm 1 with $\text{type} \in \{\text{approx}, \text{detail}\}$ and $f_{\text{approx}} = g$, $f_{\text{detail}} = h$.

$$y_{\text{type}}[n] = \sum_{k=-\infty}^{\infty} x[k] f_{\text{type}}[2n - k] \quad (2)$$

To obtain multi-scale representations of the original signal, the operation for $x[n]$ is recursively applied to y_a (approx) to derive level 2 wavelet coefficients y_a^2 and y_d^2 (detail). Here, $x[n]$ represents intermediate signals across the context length at each decoder block output in the LLM. The approximate coefficients y_a and y_d , along with their decompositions $\{y_a, y_d, y_a^2, y_d^2, y_a^3, y_d^3, \dots\}$, are used for further processing. Notably, $y_a^2, y_d^2, y_a^3, y_d^3$ have lengths reduced by factors of 2, 4, 8, . . . The Haar wavelet transform averages adjacent samples while preserving causality by averaging current and past samples. Higher-order coefficients capture averages over larger context lengths, as shown in Figure 2. We can continue until only a single scalar value remains, representing the mean of the signal. The Haar wavelet transform computes averages and differences to create a multi-resolution representation, capturing low and high frequencies at different resolutions. Figure 2 illustrates the same signal captured at coarser and finer representations using Haar wavelets, applied to intermediate embeddings, allowing each next token prediction access to these representations. For the case of learnable wavelet kernels, we create a multi-resolution representation by varying the kernel size (Algorithm 1) to allow the LLM to learn the optimal kernels optimized for the next token prediction.

3.1. Connecting wavelets and LLM embeddings

In many signal processing applications, first order detailed along with approximate coefficients captures signals at various levels. We do the same with signals from intermediate transformer embeddings across tokens. Our premise is that real-world data is structured: text ranges from letters to words, sentences, and topics, symbolic music ranges from notes, motifs and pieces with speech from phonemes, morphemes to syllables to phrases. With Haar wavelet, this can be approximated as a simple averaging operation. For the learnable version, the weights of the kernel for the multi-scale version are optimized to predict the next token. Continuing with the approximate coefficients will eventually yield a single scalar, the average of the entire signal in the case of the Haar wavelet. Several methods can be employed to match the original signal’s sequence length from the approximation coefficients, including up-sampling. We refer to the signal approximated at a specific level with the same length as the “approximate signal” distinguishing it from shorter approximate coefficients. In Figure 2 (R), to obtain the signal approximation at various levels matching the original

Algorithm 1 Wavelet-GPT

```

1:  $E$ : Model or Embedding Dimension
2:  $L$ : Context Length
3:  $N + 1$ : Number of Decoder Layers
4: for layer  $l = 1, 2, \dots, N$  do
5:    $\mathbf{x}^l \leftarrow$  Output of the  $l$ -th Decoder, dimension:  $E \times L$ 
6:    $\mathbf{xn}^l \leftarrow$  Modified decoder embedding replacing  $\mathbf{x}^l$ 
7:    $\mathbf{xn}_{(i)}^l \leftarrow \mathbf{x}_{(i)}^l$  for embedding dimension  $i < E/2$ 
8:    $f(i) \leftarrow 2^F$   $F = \text{int}((L_k * (i - E/2)) / (E/2 - 1))$ 
9:    $L_k = \lfloor \log_2(L) \rfloor + 1$   $i \geq E/2$ 
10:  // Kernel length function of embd coordinate power of 2
11:   $\mathbf{xn}_{(i)}^l(k) \leftarrow \frac{1}{f(i)} \sum_{m=k-f(i)}^k \mathbf{x}_{(i)}^l(m)$   $i \geq E/2$ 
12:  // for non-learnable fixed Haar wavelet
13:   $\mathbf{xn}_{(i)}^l(k) \leftarrow \sum_{m=0}^{f(i)-1} h(m) \cdot \mathbf{x}_{(i)}^l(k - m)$   $i \geq E/2$ 
14:  // for learnable wavelet kernel  $h$ 
15: end for

```

input signal $x[n]$, we apply the wavelet kernel by multiplying the approximate coefficients with the kernel for that level (e.g., $[1, 1]$, $[1, 1, 1, 1]$, etc.). This piecewise constant function is shown in Figure 2. LLM embedding coordinates define unique resolution kernels, each corresponding to a specific scale of data. The reconstructed signal $x_{\text{recon}}[n]$, a method to derive the *approximate signal*, is computed from wavelet coefficients c_j at level j as:

$$x_{\text{recon}}^j[n] = \sum_k c_k \cdot \psi_{j,k}[n] \quad (3)$$

Equation 3 requires storing child wavelets at various approximations, complicating the process and rendering it non-causal as computing c_k considers the entire signal. Due to the dependence of c_k on future information, we cannot use this to reconstruct the signal from its approximate coefficients. To adapt this for LLM, we simplify the computation of the *approximate signal* in a differentiable manner using a variant from Equation 3 in both multi-resolution learnable/non-learnable kernel settings. For the Haar wavelet, we compute an average of the input signal with varying kernel lengths, increasing the length until it approximates the entire signal. The kernel length determines the level of signal approximation. LLMs operate under a causality assumption, modifying the signal at a location using prior samples within the kernel length. We zero-pad the signal to the left when the window length is shorter than the kernel. Wavelet transform at different levels gives several versions of the signal at different resolutions, which can mess up the structure of the intermediate embeddings. To address this, we create different resolutions for signal approximations parameterized by embedding dimension. In Section 4.4, we make these kernels learnable, allowing the architecture to maintain multi-scale operation (Equation 3), with learnable weights with $x_{\text{recon}}[n]$ now being learned with resolution parameterized by latent dimension.

3.2. Wavelet Coefficients by Embedding Coordinates

One option is to compute the *approximate signals* for each coordinate signal $x_{(i)}^l$ across all decoder layers at levels I to IX. For a context length of 512, this would require nine additional signals with resolutions of 512, 256, 128, 64, 32, 16, 8, 4, and 2, significantly increasing complexity and necessitating major modifications to our GPT model. We propose a novel solution to address this. Instead of computing all levels of *approximate signals* for every intermediate embedding dimension, we parameterize the level by the embedding dimension index. We want to steer the embeddings only a little into the inductive biases we impose to avoid too much tinkering with what they learn. Transformers have been wildly successful without incorporating any inductive biases. Ideally, we want the best of both worlds, nudging intermediate GPT embeddings in only half of the dimensions. We adjust intermediate GPT embeddings in only half the dimensions. Embeddings from 0 to $E/2$ (coordinates 0 to 64 when $E = 128$) remain unchanged. For the rest, we apply processing based on their index i . If $x_{(i)}^l$ is an intermediate embedding after the l^{th} decoder layer along the i^{th} dimension, the modified signal $xn_{(i)}^l$ equals $x_{(i)}^l$ for $i \in [0, E/2]$. For $i > E/2$, we impose structure using an approximate signal calculated from wavelet coefficients corresponding to the index i . We use a mapping function f that takes coordinate i (ranging from $E/2$ to E) and returns the kernel size corresponding to approximation levels from I to IX. The linear function gradually increases from level I (kernel size two at $i = E/2$) to level IX (kernel size 512 at $i = E$, or the coarsest representation i.e., a scalar).

Now, let us find out how we compute the modified new signal $xn_{(i)}^l$ that replaces the original intermediate Transformer embeddings $x_{(i)}^l$. $f(i)$ is the kernel size for the coordinate i . The modified signal is either kept the same or modified as $xn_{(i)}^l(k) = \frac{1}{f(i)} \sum_{m=k-f(i)}^k x_{(i)}^l(m)$ as seen in Algorithm 1. For cases where $k - f(i) < 0$, we zero-pad the signal to ensure valid average/kernel computation. Specifically, for the Haar wavelet, the modified signal acts as a causal moving average filter with finite length, averaging the embedding signal along the i^{th} coordinate with a kernel size determined by $f(i)$. This operation does not introduce new parameters or maintain causality in LLMs to prevent future token leakage, as seen in Equation 4. In Algorithm 1, each value of the modified signal at token k is computed using a convolution with a learned kernel $h(\cdot)$ and variable length $f(i)$, parameterized by the embedding coordinate dimension i . Each kernel is learned independently for every signal.

3.3. Imposing Structure: Toy Example

In Figure 3, we illustrate a toy example of how we impose structure onto decoder Transformer embeddings. The left side shows eight variations along the token dimension, with

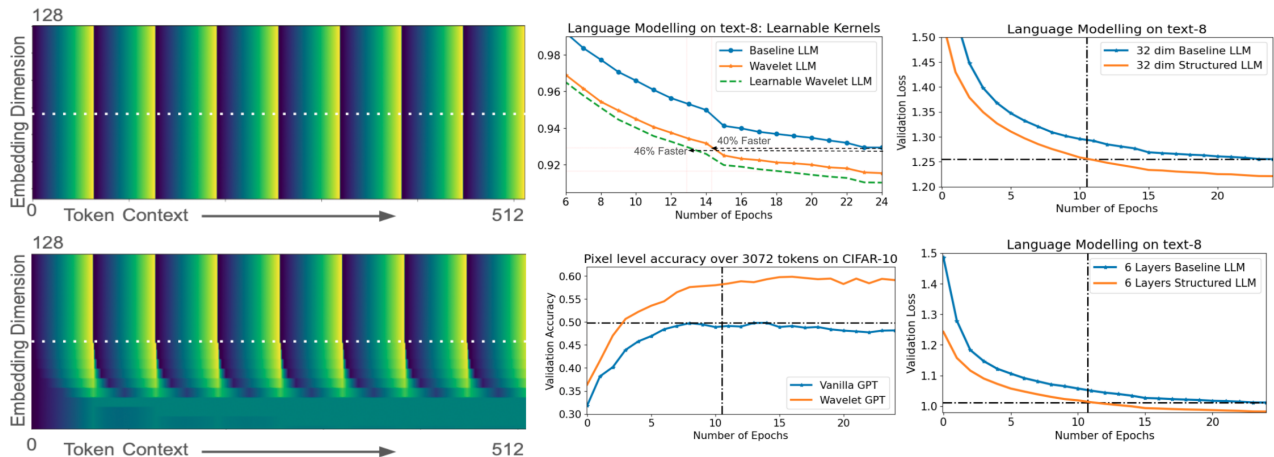


Figure 3. (Left) Toy example showing embeddings before/after imposing multi-rate structure. Different embedding dimensions advance at distinct rates while maintaining causality, as seen from patterns dispersing from dimension 64 to 0. (Right) Validation loss during pre-training on text-8 with learnable multi-scale structure achieving comparable performance nearly twice as fast/performance boost akin to adding additional decoder layers. Our architecture’s performance on text-8 with a 32-dim model matches the speedup similar to that seen for 128-dim and shallower models. LRA image benchmark, a 10% performance increase without adding any parameters

onset/sudden bursts at token indices 32, 64, etc., decreasing to zero before rising again. As discussed in the introduction, datasets inherently possess a hierarchical structure, which we capture by imposing intermediate Transformer embeddings at each layer. In this example, we retain embeddings at the original resolution for half the dimensions (split by a white line). For the other half, we gradually increase the kernel length across the context and compute the average causally. The final embedding dimension averages over the token dimension with a kernel size equal to the context length (zero-padding if necessary). This creates highways, allowing embeddings to move at different rates: the coordinates from $E/2$ to E move at the Transformer’s original speed, while those from 0 to $E/2$ transition from faster to slower movement. This approach enables the attention mechanism to utilize multi-scale features at varying rates across all layers and tokens, as explored in the next section. Further, this multi-scale structure can be made learnable, driven by just the next token prediction.

4. Experiments

The main aim of these experiments is to show that the pre-training performance of the models across four modalities improves with/without doing intermediate modifications on embeddings inspired by wavelets. We also benchmark on LRA tasks. We propose a shrunk-down GPT baseline architecture that has the same topology. We do not compare against larger architectures, as this paper focuses on pre-training from scratch, and was written in with access to limited computational resources in academia. We evaluate pre-training performance with and without wavelet-inspired blocks. We only report how well our generative model

does for pretraining by quantifying the likelihood scores similar to papers such as Mega-Byte (Yu et al., 2023) and Music Transformer (Huang et al., 2019) that only report NLL scores in the entire paper. We also validate our method across various modalities such as text, audio and music. Further, we benchmark it on various input representations such as raw waveform, MIDI tokens, acoustic tokens, text bytes, characters, and BPE tokens, in addition to math expressions. Our experiments, based on the GPT-2 architecture, have 10 Transformer decoder layers with a context length of 512, trained from scratch. Each modality shares the same architecture, using an embedding dimension of 128, a feed-forward dimension of 512, and 8 attention heads. The final decoder outputs a dense layer of 2048 neurons, followed by a layer matching the vocabulary size². Baseline models consist of standard Transformer decoder blocks without modified embeddings. We retain half³ of the embedding coordinates for our proposed architecture and impose either a fixed or learnable multi-scale structure on the other half for all intermediate layers. All models were trained from scratch in TensorFlow (Abadi et al., 2016) for 25 epochs, starting with a learning rate of $3e-4$, decreasing to $1e-5$ when loss plateaued. Each model utilized 1M training points, totalling 500 million tokens, randomly cropped from the dataset. We measured performance using negative log-likelihood loss, as this method improves the core architecture of the

²Vocab of 27 for text8, 256 for raw waveform (Goel et al., 2022; Verma, 2022), 388 for symbolic music, and 1024 for ENCODEC speech tokens, 256 for 8-bit raw pixels, 50257 for BPE tokens

³The choice of half is a hyper-parameter and it is difficult to optimize for every modality and input representation due to computational resource constraints. If the optimal split is not half, it will only improve the already strong results

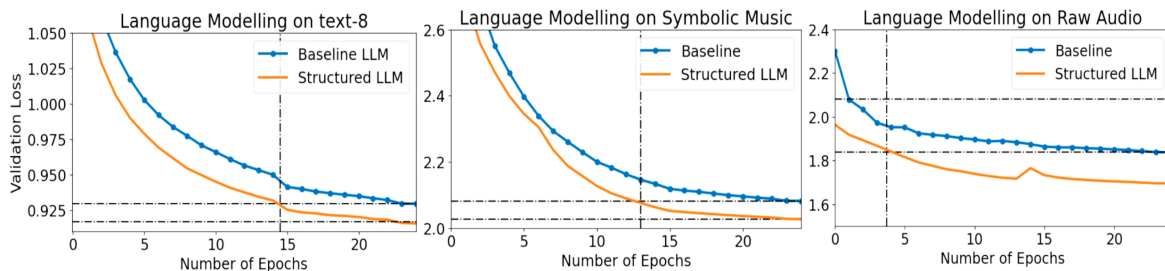


Figure 4. Results for natural language, symbolic music, and raw audio. We perform faster than baseline, almost twice as fast on shrunk-down GPT. We see substantial gains in pre-training performance for the same epochs, equivalent to a much larger architecture. The black vertical line denotes the epoch at which our architecture achieves the same performance as our baseline architecture.

transformer-based GPT - helping achieve the objective we want to achieve: predict the next token correctly. Since we are operating on intermediate embeddings, our work can hopefully generalize to setups with structured data similar to text, raw audio, and symbolic music, where one can go from a fine-grained structure to a coarse structure. We impose a multi-scale structure that allows the attention mechanism to learn dependencies across embeddings and inject some information that can capture coarse and fine-grained structures into embedding coordinates while maintaining causality.

4.1. Performance on modalities

We compared the performance of our baseline architecture across three modalities : text, symbolic music, and audio waveform with and without wavelet-based intermediate operations. Results showed significant performance improvements in all modalities with the same number of training steps. To illustrate, a 0.04 decrease in validation loss is comparable to going from a 16 to a 64-layer model on text-8 dataset (papers-with code, 2024). As shown in Figure 4, our modified GPT architecture achieves this loss nearly twice as quickly in training steps as the original model, showing that GPT-like architecture can take advantage of the structure we imposed on half of the embedding dimensions. This speedup, i.e., the number of epochs/steps taken to achieve the same performance (SP: same performance epoch), is even smaller for raw audio due to the quasi-stationary nature of audio signals at smaller time scales (20-30 ms for harmonic sounds). For a sampling rate of 16KHz, a context length of 512 would correspond to 32ms, which may be one of the reasons that some of the coordinates nail down the contents of the context in fewer coordinates onto which we impose structure. The convergence is significantly faster for the raw waveform LLM setup and achieves nearly twice the speed of text-8 and symbolic music. We also ran benchmarks on LibriSpeech corpus about 1000 hours of speech and acoustic tokens, further strengthening our method is generic to handle several types and modalities of tokens. We run our method on audio classification with Audio Transformer over 200 categories of audio for FSD-50K

benchmarks (Fonseca et. al, 2020). We get a performance boost and speedups, thereby showcasing the ubiquity of our proposed method for generative modelling and classification as well. We also compare the absolute clock run times of our modifications in both learnable/non-learnable setups. Table 1 reports the time to complete one epoch relative to our baseline architecture. Our method is computationally inexpensive, as it only involves fixed kernel multiplication or learning a single filter convolutional kernel with variable context lengths along different coordinates.

4.2. Making multi-scale kernels learnable

We allow each kernel to be learnable. In the previous section, we defined the shape of the kernel and computed approximate signals of intermediate layer activations across all layers, with different resolutions occurring at different embedding dimensions to mimic a causal version of the wavelet transform. Now, we allow each kernel of length L at a particular level to be learnable for computing the *approximate signal* for various resolutions, yet another way to compute it. By making the computation of approximate signal learnable, the model can learn how to weight every decoder layer dimension instead of putting a fixed kernel, e.g. exponentially weighted average. This as can be seen, Algorithm 1 only allows 20k or 0.2 % extra parameters to our base decoder architecture. We run the experiments both for learnable kernels and fixed kernels (three for each case) due to scarcity of resources. Intuitively there will exist an optimal kernel whose shape is best optimized for the next token prediction for a specific modality of interest than simple Haar wavelet. This further improves our performance from 42% to 48% faster speedup to get a similar baseline performance, seen in Figure 4, carried out on the text-8. We also benchmark on Wiki-103 to demonstrate that our method works with the GPT-2 tokenizer giving even larger gains. As shown in Figure 5, we match the performance of a 10-layer architecture at more than twice the speed. In addition to faster convergence, we see a 3.6-point improvement in perplexity scores over the baseline model for Wiki-103. Section 4.4 shows we scale with model size and depth showing promise

Modality	Baseline	Proposed	SPE	SpeedUp	Rel. GPU Hrs
Text-8	0.93	0.92	14.5	42%	1.013
Raw Audio	1.84	1.70	3.7	85%	1.042
Symbolic Music	2.08	2.02	13	48%	1.059
Text-8 (L)	0.93	0.91	12.9	48%	1.094
Wiki-103 (L)	4.11	4.05	9.5	62%	1.130
LibriSpeech (L)	2.43	2.40	9.2	63%	1.110
FSD-50K	40.6%	42.8%	32	65%	1.037

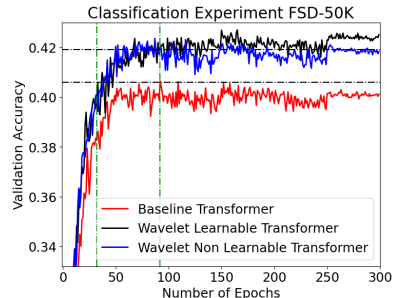


Figure 5. Comparison of the negative-log likelihood (NLL) scores for our architecture across three modalities, with and without wavelet-based fixed/learnable (L) structure. (Left) Table shows the NLL scores and speedup, with Same Performance Epoch (SPE) with baseline as 25 epochs, relative GPU hours. (R) FSD-50K Audio Transformer top-5 accuracy results. Vertical green lines indicate the highest accuracy achieved and the point where the same accuracy is reached 60% faster using our proposed method, with no extra parameters.

for improvements in larger LLM architectures.

4.3. Ablation on Depth And Model Dimension

The aim for these experiments was to see if our model scales with depth of the Transformer and the model dimension. We explore two architecture variants on text-8: (i) reducing the model dimension from 128 to 32 and (ii) reducing the number of layers. The model with 32-dimensional, 10 decoder layers (eight heads) achieves baseline performance in around ten epochs and runs nearly twice as fast (Figure 4). For the second experiment, we retain the architecture from Table 1 but reduce the Transformer decoder to six layers while keeping other parameters unchanged (feed-forward dimension four times the model dimension, eight heads). With Haar-inspired modifications, the model matches baseline performance twice as fast, consistent with the results reported in Section 4.1. While it is difficult to scale the architectures beyond a certain depth and model dimension in academic setups: we believe that by seeing the effect of model dimension and depth holding, we are confident that the findings will extrapolate for much larger/deeper models.

4.4. Audio Classification Benchmark

We explore the strength of our method for a typical audio classification on a standard audio classification benchmark FSD-50K. The goal is to identify the sound categories in 1s of audio correctly. We use a transformer-based architecture similar to Audio Transformer as our baseline model. It consists of 128 convolutional filters with a length of 200 learned over 25ms of audio sampled at 16KHz, yielding patches of 400-length audio samples. The convolutional filter output is then max-pooled across the 25ms window to give a single vector of length 128, i.e. the number of convolutional filters being fed to a Transformer stack of 6 layers with model dimension as 64 similar to (Verma & Chafe, 2023; Verma & Berger, 2021). We report on the top-5 % accuracy and relative gain in mAP scores for our proposed architecture with learnable/non-learnable kernels. We see that we get a performance boost of about 2% and a

faster convergence of more than 60%, as reported in Figure 5, for the learnable/fixed kernels and baseline.

4.5. Similarities and Differences With EMA

We compare Exponential Moving Averages (EMA) on intermediate signals. Unlike the Haar wavelet, which takes fixed window weights, which takes the mean of the signal in the window, EMA uses an exponential kernel. Let the signal $x_i^l(t)$, after the l^{th} layer, be of length equal to context length, with t being the token index from 0 to L at embedding dimension i . The modified signal s_t is: $s_0 = x_i^l(0)$ $s_t = \alpha x_i^l(t) + (1 - \alpha)s_{t-1}$ where α , the decay factor, satisfies $0 < \alpha < 1$. Unlike an EMA, our method captures multi-scale information using a finite kernel with zero weights outside a specified length. In text-8 experiments, we applied EMA on half of the embedding dimensions, with α linearly varying between 0 and 1 for dimensions 64 to 128 mimicing our approach with a classical approach. This under-performed compared to our baseline, with an NLL score of 0.94, while our baseline and proposed method achieved scores of 0.93, 0.92, and 0.91 for non-learnable and learnable cases, respectively. Our method provides a simple, signal processing-based scheme that optimizes weights across multiple resolutions driven by next-token prediction and outperforms EMA. Depending on α , the EMA filter produces an exponential kernel while we maintain a constant kernel or allow weights learned from scratch optimized for the next token prediction. Further, EMA is an Infinite-Impulse Response (IIR) filter, whereas the Haar wavelet-based kernel is a Finite Impulse Response (FIR) filter. Consequently, for each value update, the contributions from previous samples never reach zero. These can accumulate significantly at longer context lengths for certain α . The recursive, non-learnable nature of the EMA IIR filter ensures some contribution from all embeddings, which explains performance degradation. In contrast, our method uses zero weights outside the kernel length, capturing multi-scale information.

Table 1. Performance on LRA tasks ((Tay et al., 2020b)) as reported in (Liu et al., 2024). Bold the best-performing model, and underlined indicates the second-best. We use a baseline GPT baseline (Section 5) and modify intermediate embeddings by imposing a hierarchical structure. Non-transformer-based, modified attention-based or hybrid architectures are not reported.

Attention Based Models	ListOps	Text	Image
Transformer (Vaswani et al., 2017)	36.37	64.27	42.44
Local Attention (Tay et al., 2020b)	15.82	63.98	41.46
Linear Trans. (Vyas et al., 2020)	16.13	<u>65.90</u>	42.34
Linformer (Wang et al., 2020)	35.70	53.94	38.56
Sparse Trans. (Child et al., 2019)	17.07	63.58	44.24
Performer (Kaiser et al., 2021)	18.01	65.40	42.77
Sinkhorn (Tay et al., 2020a)	33.67	61.20	41.23
Longformer (Beltagy et al., 2020)	35.63	64.02	40.83
BigBird (Zaheer et al., 2020)	36.05	64.02	40.83
Luna-256 (Ma et al., 2021)	37.25	65.78	47.86
Reformer (Kitaev et al., 2020)	37.27	56.10	38.07
Non-Causal			
FNET (Lee-Thorp et al., 2022)	37.27	56.10	38.07
WavSPA (Zhuang et al., 2024)	<u>55.40</u>	81.60	<u>55.58</u>
(Ours) GPT Baseline	41.65	65.32	49.81
(Ours) WaveletGPT	57.5	<u>66.38</u>	59.81

5. Long Range Arena Benchmarks

We adapt our architecture for Long-Range Arena (LRA) tasks (Tay et al., 2021), testing on long-range prediction across text, images, and mathematical expressions. These tasks evaluate the model’s ability to handle similarity, structure, and reasoning over extended contexts. We focus on transformer-based architectures, as recently reported by (Liu et al., 2024), while other variants include state-space, hybrid models or tweaking attention mechanisms. For text, we perform binary classification on the IMDb review dataset (Maas et al., 2011) using byte-level data with a context length of 2048 to determine if a movie review is positive or negative. We use CIFAR-10 from the LRA benchmark for images, classifying sequences of 3072 pixels into one of ten categories. Lastly, we benchmark on Long ListOps, testing the model’s ability to understand hierarchically structured data in extended contexts. In our task, we use a version of ListOps of sequence lengths of up to 2K to test the ability to reason hierarchically while handling long contexts. The model needs to access all tokens and model the logical structure of the inputs to make a prediction. The task is a ten-way classification task and is considerably challenging. We use the setup provided by (Khalitov et al., 2022) to extract the data and be uniform with other benchmarks. We use identical architecture for all three modalities, only modifying the embedding matrix to accommodate different tokenizers and output categories. Our baseline consists of a 6-layer causal Transformer decoder with a model dimension of 32 and a feed-forward dimension four times that of the embedding dimension. We extract the last token of the sequence as a

32-dimensional embedding for classification, followed by a dense layer with 2048 neurons and a final dense layer corresponding to the number of categories. The input goes through an embedding layer that converts discrete tokens into a 32-dimensional vector. The input vocabularies are 256 for text/image and 16 for ListOps. The context lengths are 2048, 3072, and 1999 tokens, with 2, 10, and 10 as output categories. In our modified architecture, we introduce our waveletGPT module between each decoder layer, retaining half of the embedding dimensions as they are. For the other half, we use non-learnable kernels, increasing the kernel size from 2, 4, and 8 to 512 linearly for dimensions 16 to 32 while maintaining the causality assumption. This introduces highways that hierarchically process data at each embedding and Transformer decoder layer without adding parameters, similar to our approach for pre-trained LLM. As shown in Table 1, we achieve notable gains across all three modalities, where even minor improvements are worth reporting. We significantly outperform non-causal signal processing based methods, such as (Zhuang et al., 2024), with nearly 2% improvement on ListOps and 4.5% on a much smaller architecture: ours has 32 dimensions and six layers compared to 128 dimensions/eight layers. We limit our comparison method for fairness only with vanilla Transformer architectures. We also compare two non-causal architectures incorporating signal processing-based ideas: FNET and WavSPA. Compared to non-causal FNet, our model significantly outperformed all three LRA tasks, achieving 20% improvement on ListOps and Image and 10% on text. The most notable gain is in the ListOps task, which involves modelling a hierarchical, tree-like structure of math operations, making our model particularly suitable. To the best of our knowledge (Liu et al., 2024), this is the best result by a simple attention-based Transformer on LRA tasks.

6. Conclusion and Future Work

We showcase a powerful incorporation of a core signal processing idea, namely wavelets, into large language model pre-training. By imposing a multi-scale structure onto every intermediate embedding, we achieve the same performance 40-60% faster than a baseline architecture without adding any parameters. We achieve a substantial performance boost if we train for the same number of steps. Further we show strong gains in LRA benchmarks without adding any parameters by giving every next token prediction access to multi-scale embeddings in every decoder layer. Our method generalizes across three modalities: raw text, symbolic music, and raw audio, giving similar performance speedups on several input representations, namely raw audio samples, acoustic tokens, MIDI tokens, byte text, math expressions, BPE tokens for text, raw image pixels and characters. This shows it is generic enough for improving pre-training performance across datasets and input representations.

7. Acknowledgment

This work was supported by the Stanford Institute of Human-Centered AI (Stanford-HAI) through a Google Cloud computing grant for the academic year 2023. The author is thankful to Prof. Dan Jurafsky for feedback and helpful discussions on the problem and its impact on the field.

References

- Abadi, M., Barham, P., Chen, J., Chen, Z., Davis, A., Dean, J., Devin, M., Ghemawat, S., Irving, G., Isard, M., et al. {TensorFlow}: A system for {Large-Scale} machine learning. In *12th USENIX symposium on operating systems design and implementation (OSDI 16)*, pp. 265–283, 2016.
- Ahmed, N., Natarajan, T., and Rao, K. R. Discrete cosine transform. *IEEE transactions on Computers*, 100(1):90–93, 1974.
- Al-Rfou, R., Choe, D., Constant, N., Guo, M., and Jones, L. Character-level language modeling with deeper self-attention. In *Proceedings of the AAAI conference on artificial intelligence*, volume 33, pp. 3159–3166, 2019.
- Beltagy, I., Peters, M. E., and Cohan, A. Longformer: The long-document transformer. In *Proceedings of the 2020 Conference on Empirical Methods in Natural Language Processing (EMNLP)*, pp. 6150–6160, 2020. URL <https://www.aclweb.org/anthology/2020.emnlp-main.519/>.
- Borsos, Z., Marinier, R., Vincent, D., Kharitonov, E., Pietquin, O., Sharifi, M., Roblek, D., Teboul, O., Grangier, D., Tagliasacchi, M., et al. Audioldm: a language modeling approach to audio generation. *IEEE/ACM Transactions on Audio, Speech, and Language Processing*, 2023.
- Brohan, A., Brown, N., Carbajal, J., Chebotar, Y., Chen, X., Choremanski, K., Ding, T., Driess, D., Dubey, A., Finn, C., et al. Rt-2: Vision-language-action models transfer web knowledge to robotic control. *arXiv preprint arXiv:2307.15818*, 2023a.
- Brohan, A., Brown, N., Carbajal, J., Chebotar, Y., Dabis, J., Finn, C., Gopalakrishnan, K., Hausman, K., Herzog, A., Hsu, J., et al. Rt-1: Robotics transformer for real-world control at scale. In *Robotics: Science and Systems*. RSS, 2023b.
- Brown et, al, T. Language models are few-shot learners. *arXiv preprint arXiv:2005.14165*, 2020.
- Caucheteux, C., Gramfort, A., and King, J.-R. Evidence of a predictive coding hierarchy in the human brain listening to speech. *Nature human behaviour*, 7(3):430–441, 2023.
- Child, R., Elsen, E., Kim, D., and Hinton, G. Sparse transformer. In *Proceedings of the 33rd Conference on Neural Information Processing Systems (NeurIPS 2019)*, 2019. URL <https://arxiv.org/abs/1904.10509>.
- Défossez, A., Copet, J., Synnaeve, G., and Adi, Y. High fidelity neural audio compression. *arXiv preprint arXiv:2210.13438*, 2022.
- Dettmers, T., Pagnoni, A., Holtzman, A., and Zettlemoyer, L. Qlora: Efficient finetuning of quantized llms. *Advances in Neural Information Processing Systems*, 36, 2024.
- Devlin, J., Chang, M.-W., Lee, K., and Toutanova, K. Bert: Pre-training of deep bidirectional transformers for language understanding. In *Proceedings of the 2019 Conference of the North American Chapter of the Association for Computational Linguistics*, 2019.
- Dosovitskiy, A., Beyer, L., Kolesnikov, A., Weissenborn, D., Zhai, X., Unterthiner, T., Dehghani, M., Bischof, H., and Schiele, B. An image is worth 16x16 words: Transformers for image recognition at scale. In *Proceedings of the International Conference on Learning Representations (ICLR)*, 2021. URL <https://openreview.net/forum?id=Yg6M6i5Zx0>.
- Fedus, W., Zoph, B., and Shazeer, N. Switch transformers: Scaling to trillion parameter models with simple and efficient sparsity. *Journal of Machine Learning Research*, 23(120):1–39, 2022.
- Flores-Mangas, F. Discrete wavelet transform. *The Washington Post*, Spring 2014. URL <https://www.cs.toronto.edu/~mangas/teaching/320/slides/CSC320L11.pdf>.
- Fonseca et. al, E. Fsd50k: an open dataset of human-labeled sound events. *arXiv preprint arXiv:2010.00475*, 2020.
- Gao, R. X. and Yan, R. Non-stationary signal processing for bearing health monitoring. *International journal of manufacturing research*, 1(1):18–40, 2006.
- Goel, K., Gu, A., Donahue, C., and Ré, C. It’s raw! audio generation with state-space models. In *International Conference on Machine Learning*, pp. 7616–7633. PMLR, 2022.
- Gu, Y., Dong, L., Wei, F., and Huang, M. MiniLLM: Knowledge distillation of large language models. In *The Twelfth International Conference on Learning Representations*, 2024. URL <https://openreview.net/forum?id=5h0qf7IBZZ>.
- Hawthorne, C., Stasyuk, A., Roberts, A., Simon, I., Huang, C.-Z. A., Dieleman, S., Elsen, E., Engel, J., and Eck, D. Enabling factorized piano music modeling and generation

- with the maestro dataset. In *Proceedings of the International Conference on Learning Representations (ICLR)*, 2019. URL <https://openreview.net/forum?id=H1gJq2R5K7>.
- He et. al, K. Deep residual learning for image recognition. In *Proceedings of the IEEE conference on computer vision and pattern recognition*, pp. 770, 2016.
- Hinton, G., Vinyals, O., and Dean, J. Distilling the knowledge in a neural network. *arXiv preprint arXiv:1503.02531*, abs/1503.02531, 2015. URL <http://arxiv.org/abs/1503.02531>.
- Huang, C.-Z. A., Vaswani, A., Uszkoreit, J., Shazeer, N., Simon, I., Hawthorne, C., Dai, A. M., Hoffman, M. D., Dinculescu, M., and Eck, D. Music transformer: Generating music with long-term structure. In *International Conference on Learning Representations (ICLR)*, 2019. URL <https://openreview.net/forum?id=rJe4ShAcF7>.
- Huang, K. and Aviyente, S. Wavelet feature selection for image classification. *IEEE Transactions on Image Processing*, 17(9):1709–1720, 2008.
- Kaiser, L., Likhoshesterov, V., Dohan, D., Song, X., Gane, A., Sarlos, T., Hawkins, P., Davis, J., Mohiuddin, A., , Belanger, D., Choromanski, K., Colwell, L., and Weller, A. Rethinking attention with performers. In *Proceedings of the 9th International Conference on Learning Representations (ICLR)*, 2021. URL <https://openreview.net/forum?id=Ua6zuk0WRH>.
- Khalitov, R., Yu, T., Cheng, L., and Yang, Z. Sparse factorization of square matrices with application to neural attention modeling. *Neural Networks*, 152:160–168, 2022.
- Kingsbury, N. and Magarey, J. Wavelet transforms in image processing, 1998.
- Kitaev, N., Kaiser, Ł., and Levskaya, A. Reformer: The efficient transformer. In *Proceedings of the 8th International Conference on Learning Representations (ICLR)*, 2020. URL <https://openreview.net/forum?id=rkgNKkHtvB>.
- Koutnik, J., Greff, K., Gomez, F., and Schmidhuber, J. A clockwork rnn. In *International conference on machine learning*, pp. 1863–1871. PMLR, 2014.
- Langley, P. Crafting papers on machine learning. In Langley, P. (ed.), *Proceedings of the 17th International Conference on Machine Learning (ICML 2000)*, pp. 1207–1216, Stanford, CA, 2000. Morgan Kaufmann.
- Lee-Thorp, J., Ainslie, J., Eckstein, I., and Ontanon, S. FNet: Mixing tokens with Fourier transforms. In Carpuat, M., de Marneffe, M.-C., and Meza Ruiz, I. V. (eds.), *Proceedings of the 2022 Conference of the North American Chapter of the Association for Computational Linguistics: Human Language Technologies*, pp. 4296–4313, Seattle, United States, July 2022. Association for Computational Linguistics. doi: 10.18653/v1/2022.naacl-main.319. URL <https://aclanthology.org/2022.naacl-main.319>.
- Liu, Z., Li, S., Wang, L., Wang, Z., Liu, Y., and Li, S. Z. Short-long convolutions help hardware-efficient linear attention to focus on long sequences. *arXiv preprint arXiv:2406.08128*, 2024.
- Ma, X., Kong, X., Wang, S., Zhou, C., May, J., Ma, H., and Zettlemoyer, L. Luna: Linear unified nested attention. In *Advances in Neural Information Processing Systems 34 (NeurIPS 2021)*, pp. 1235–1246, 2021. URL <https://proceedings.neurips.cc/paper/2021/hash/14319d9cfc6123106878dc20b94fbaf3-Abstract.html>.
- Maas, A. L., Daly, R. E., Pham, P. T., Huang, D., Ng, A. Y., and Potts, C. Learning word vectors for sentiment analysis. In *Proceedings of the 49th Annual Meeting of the Association for Computational Linguistics: Human Language Technologies*, pp. 142–150, Portland, Oregon, USA, June 2011. Association for Computational Linguistics. URL <http://www.aclweb.org/anthology/P11-1015>.
- Madani, A., McCann, B., Naik, N., Keskar, N. S., Anand, N., Eguchi, R. R., Huang, P.-S., and Socher, R. Progen: Language modeling for protein generation. *NeurIPS workshop on ML For Structural Biology*, 2020.
- Mikolov, T., Sutskever, I., Deoras, A., Le, H.-S., Kombrink, S., and Cernocky, J. Subword language modeling with neural networks. *preprint (http://www.fit.vutbr.cz/~mikolov/rnnlm/char.pdf)*, 8(67), 2012.
- Nawrot, P., Tworkowski, S., Tyrolski, M., Kaiser, L., Wu, Y., Szegedy, C., and Michalewski, H. Hierarchical transformers are more efficient language models. In Carpuat, M., de Marneffe, M.-C., and Meza Ruiz, I. V. (eds.), *Findings of the Association for Computational Linguistics: NAACL 2022*, pp. 1559–1571, Seattle, United States, July 2022. Association for Computational Linguistics. doi: 10.18653/v1/2022.findings-naacl.117. URL <https://aclanthology.org/2022.findings-naacl.117>.
- Nix, N. Silicon valley is pricing academics out of ai research. *The Washington Post*, March 2024. URL <https://www.washingtonpost.com>.

- com/technology/2024/03/10/big-tech-companies-ai-research/
- papers-with code. Language modelling on text8. March 2024. URL <https://paperswithcode.com/sota/language-modelling-on-text8>.
- Selva, J., Johansen, A. S., Escalera, S., Nasrollahi, K., Moeslund, T. B., and Clapés, A. Video transformers: A survey. *IEEE Transactions on Pattern Analysis and Machine Intelligence*, 2023.
- Sun, M., Liu, Z., Bair, A., and Kolter, J. Z. A simple and effective pruning approach for large language models. In *The Twelfth International Conference on Learning Representations*, 2024. URL <https://openreview.net/forum?id=PxoFut3dWW>.
- Tamkin et. al, A. Language through a prism: A spectral approach for multiscale language representations. *Advances in Neural Information Processing Systems*, 33, 2020.
- Tay, Y., Metzler, D., Zhao, X., and Zheng, S. Sinkhorn transformer: Generating long-form text via randomized greedy sorting. In *Proceedings of the 37th International Conference on Machine Learning (ICML)*, pp. 9408–9419, 2020a. URL <http://proceedings.mlr.press/v119/tay20a.html>.
- Tay, Y., Dehghani, M., Abnar, S., Shen, Y., Bahri, D., Pham, P., Rao, J., Yang, L., Ruder, S., and Metzler, D. Long range arena : A benchmark for efficient transformers. In *International Conference on Learning Representations*, 2021. URL <https://openreview.net/forum?id=qVyeW-grC2k>.
- Tay, Z., Dehghani, M., Vaswani, A., Shazeer, N., and Uszkoreit, J. Local attention. In *Proceedings of the International Conference on Learning Representations*, 2020b.
- Touvron, H., Lavril, T., Izacard, G., Martinet, X., Lachaux, M.-A., Lacroix, T., Rozière, B., Goyal, N., Hambro, E., Azhar, F., et al. Llama: Open and efficient foundation language models. *arXiv preprint arXiv:2302.13971*, 2023.
- Vaswani, A., Shazeer, N., Parmar, N., Uszkoreit, J., Jones, L., Gomez, A. N., Kaiser, L., and Polosukhin, I. Attention is all you need. In *Advances in neural information processing systems*, pp. 5998–6008, 2017.
- Verma, P. Goodbye wavenet—a language model for raw audio with context of 1/2 million samples. *arXiv preprint arXiv:2206.08297*, 2022.
- Verma, P. and Berger, J. Audio transformers: Transformer architectures for large scale audio understanding. *arXiv preprint arXiv:2105.00335*, 2021.
- Verma, P. and Chafe, C. A generative model for raw audio using transformer architectures. *2021 24th International Conference on Digital Audio Effects (DAFx)*, pp. 230–237, 2021. URL <https://api.semanticscholar.org/CorpusID:235683315>.
- Verma, P. and Chafe, C. A content adaptive learnable” time-frequency” representation for audio signal processing. In *ICASSP 2023*, pp. 1–5. IEEE, 2023.
- Verma, P. and Smith, J. A framework for contrastive and generative learning of audio representations. *arXiv preprint arXiv:2010.11459*, 2020.
- Vyas, A., Katharopoulos, A., Pappas, N., and Fleuret, F. Transformers are rnns: Fast autoregressive transformers with linear attention. In *Proceedings of the 37th International Conference on Machine Learning (ICML)*, pp. 5156–5165. PMLR, 2020. URL <https://arxiv.org/abs/2006.16236>.
- Wang, C., Chen, S., Wu, Y., Zhang, Z., Zhou, L., Liu, S., Chen, Z., Liu, Y., Wang, H., Li, J., et al. Neural codec language models are zero-shot text to speech synthesizers. *arXiv preprint arXiv:2301.02111*, 2023.
- Wang, S., Li, B. Z., Khabsa, M., Fang, H., and Ma, H. Linformer: Self-attention with linear complexity. *arXiv preprint arXiv:2006.04768*, 2020.
- Yan, W., Zhang, Y., Abbeel, P., and Srinivas, A. Videogpt: Video generation using vq-vae and transformers. *arXiv preprint arXiv:2104.10157*, 2021.
- Yu, L., Simig, D., Flaherty, C., Aghajanyan, A., Zettlemoyer, L., and Lewis, M. Megabyte: Predicting million-byte sequences with multiscale transformers. *Advances in Neural Information Processing Systems*, 36:78808–78823, 2023.
- Zaheer, M., Guruganesh, G., Dubey, A., Ainslie, J., Alberti, C., Ontanon, S., Pham, P., Ravula, A., Wang, Q., Yang, L., and Ahmed, A. Big bird: Transformers for longer sequences. In *Advances in Neural Information Processing Systems (NeurIPS)*, pp. 17283–17297, 2020. URL <https://proceedings.neurips.cc/paper/2020/hash/c8512d142a2d849725f31a9a7a361ab9-Abstract.html>.
- Zhuang, Y., Wang, Z., Tao, F., and Shang, J. Wavspa: Wavelet space attention for boosting transformers’ long sequence learning ability. In *Proceedings of UniReps: the First Workshop on Unifying Representations in Neural Models*, pp. 27–46. PMLR, 2024.

Impact Statement

This paper presents work whose goal is to advance the field of Machine Learning by enabling LLMs to be trained faster and pushing the performance of the smaller architectures. This will not only push the performance of the smaller architectures, but also yield faster inference. There are many potential societal consequences of our work, none which we feel must be specifically highlighted here, as it shares the same consequences in terms of positive and negative aspects of LLMs and AI systems which can potentially surpass human intelligence in near future.